Applied Nanoscience (2023) 13:5211–5230
https://doi.org/10.1007/s13204-022-02742-w

ORIGINAL ARTICLE

The influence of synthesis conditions, oligosaccharide additive and functional silane on the structure and composition of sol–gel silicas

Iryna M. Trofymchuk[1] · **Lyudmila A. Belyakova**[1]

Received: 23 February 2022 / Accepted: 9 December 2022 / Published online: 25 December 2022

Abstract

In this work, the influence of different experimental conditions on the structure and composition of silicas was elucidated. Sol–gel synthesis of silicas was realized in the presence of silica precursors (tetraethyl orthosilicate and (3-chloropropyl) triethoxysilane) as well as the β-cyclodextrin additive at various molar ratios of initial reagents. In addition, the effect of temperature on hydrolysis and condensation of silicon alkoxides (in the presence or the absence of oligosaccharide) at room temperature, 70 °C and 150 °C (hydrothermal treatment) was compared. Synthesized sol–gel silicas with different surface groups were characterized by IR spectroscopy, SEM and chemical analyses, low-temperature adsorption–desorption of nitrogen, and thermogravimetry. Chemical immobilization of functional groups on the surface of silica materials was proved by IR spectroscopy. The content of oligosaccharide moieties introduced into silicas in the process of sol–gel synthesis was estimated by acid hydrolysis of surface groups to glucose and its subsequent spectrophotometric determination. Morphology investigation was performed by SEM technique. The porous structure of synthesized silicas was elucidated by low-temperature adsorption–desorption of nitrogen. Gas-phase adsorption and liquid sorption experiments were carried out to study the role of silica's structure and composition on benzene and phenol uptake, respectively. Synthesized silicas with chloropropyl and oligosaccharide moieties demonstrate adsorption level performance of known samples and are expected to be promising for the treatment of aqueous solutions from aromatics.

Keywords Sol–gel · Silica · (3-Chloropropyl)triethoxysilane · β-Cyclodextrin · Sorption

Introduction

The synthesis of hybrid silicas is usually performed using sol–gel method, which is considered effective to modify the surface of materials. Sol–gel process is an easy, fast and low-cost method for preparation of organo-silica hybrids for different applications. Characteristics of silica materials obtained by sol–gel method depend on the experimental conditions applied (composition of the initial feedstock, variations in temperature, time, and type of treatment (like hydrothermal or microwave)). It is possible to obtain silicas with desirable structural characteristic (surface area, pore diameter, ordered or disordered pores) as well as solids with improved surface properties, which makes them widely used materials in separation, catalysis and drug delivery processes.

Increased over past years, systematic functionalization of silica has several advantages in comparison with modification by other organic/inorganic matrix (Jal et al. 2004): it is the first commercially available high specific area substrate with constant composition, enabling easy analysis and interpretation of results; immobilization on silica results in great variety of silylating agents, allowing pendant functional groups in the organic framework; active silanol groups existence on silica surface allows easier attachment of modifier than on organic polymeric or other inorganic supports; silica has high mass exchange characteristics and no swelling; it has great resistance to organic solvents and temperature.

The most common approach for hybrid silicas obtaining involves the hydrolysis and condensation of tetraethyl (TEOS) or tetramethyl orthosilicate (TMOS) precursors with different organosilanes in acidic or basic medium (Jiang

---

✉ Iryna M. Trofymchuk
trofymchuk_iryna@ukr.net

[1] Chuiko Institute of Surface Chemistry of NAS of Ukraine, 17 General Naumov Str., Kiev 03164, Ukraine

et al. 2019; Xia et al. 2019). Thus, in the synthesis of organo/inorganic hybrid materials, the addition of corresponding alkoxysilanes (halogen-, nitrogen-, sulfur-, phosphor-, alkenyl-, aryl-, epoxy-containing) and chlorosilanes (chloro- and alkylchlorosilanes) is used to incorporate organic functionalities, such as haloalkyl, amino, thiol, cyano/isocyano, vinyl/allyl, organophosphine, alkyl, or aromatic groups into the pores of the silica network (El-Nahhal and El-Ashgar 2007; Hoffmann et al. 2006; Vansant et al. 1995). The addition of functional silane and molar ratio of silicate precursors can drastically change the characteristics of sol–gel reaction solution and, as a result, potentially determine the structure and properties of the final products. In particular, tetramethoxysilane, methyltrimethoxy- and methylethoxysilane, trimethylchlorosilane, and (3-methacryloxypropyl) trimethoxysilane precursors were used for obtaining silicas, which possessed specific properties—increased hydrophilicity or hydrophobicity (depending on further use), strength, thermal stability, low dielectric constant values (Darmawan et al. 2021; Ha et al. 2008; Jiang et al. 2018; Qin et al. 2013; Wagh and Ingale 2002; Yang et al. 1997; Zhang et al. 2007). The effect of introduced organosilane on the structure and characteristics of synthesized silicas was shown with the addition of dimethyldiethoxysilan and diphenyldiethoxysilane (Wang et al. 2007, 2008a, b), hexadecyltrimethoxysilane and 3-glycidoxypropyltrimethoxysilane (Daoud et al. 2006), phenyltriethoxysilane (Kim et al. 2014), 3-chloropropyltrimethoxysilane (De Conto et al. 2018; Ghahremani et al. 2020), 3-mercaptopropyltrimethoxysilane (Richer and Mercier 2001), and others (Al-Oweini and El-Rassy 2010; Toufaily et al. 2013). The common fields of use for such hybrid silicas are biomedical applications, catalysis, materials for functional devices (sensors, solar cells), and sorption (Vansant et al. 1995; Wieszczycka et al. 2021).

Among numerous organoalkoxysilanes used for silica functionalization, (3-chloropropyl)triethoxysilane (CPTES) is still considered as one of the common as well as prospective modifiers for obtaining hybrid silica (Adam et al. 2009; Bagherzadeh et al. 2014; Edeler et al. 2019; El-Nahhal and El-Ashgar 2007; Ghorbani et al. 2021; Hello et al. 2018; Hello and Fahad 2019; Kim et al. 2001; Lanitou et al. 2007; On et al. 2001; Perez-Quintanilla et al. 2006; Vansant et al. 1995; Wang et al. 2008b; Wei et al. 2009; Wieszczycka et al. 2021; Weitkamp et al. 2001; Sahoo et al. 2007; Udayakumar et al. 2008; Xu et al. 2012). There are promising works, in which 3-chloropropyl groups obtained on the surface of sol–gel silica can be used as anchoring centers for other organic moieties (Bagherzadeh et al. 2014; Edeler et al. 2019; Ghorbani et al. 2021; Kim et al. 2001; On et al. 2001; Perez-Quintanilla et al. 2006; Sahoo et al. 2007; Udayakumar et al. 2008; Wang et al. 2008b; Weitkamp et al. 2001). Usually, such organo/inorganic hybrid silicas are used as catalysts or sorbents. However, the surface functionalization of silica with CPTES was commonly carried by its chemical immobilization to previously synthesized silica support ("grafting" method) (Bagherzadeh et al. 2014; Kim et al. 2001; Lanitou et al. 2007; On et al. 2001; Perez-Quintanilla et al. 2006; Sahoo et al. 2007; Wang et al. 2008b; Weitkamp et al. 2001;). Here, special conditions of chemical reaction for successful modification of silicas are needed (high temperatures, toxic organic solvents, lengthy refluxing time). On the contrast, chloropropyl-functionalized silicas could be prepared by simple one-pot synthesis (co-condensation method), which provides more uniform distribution of organic functionalities (Adam et al. 2009; Attol and Mihsen 2020; Udayakumar et al. 2008; Wei et al. 2009; Xu et al. 2012; Hello et al. 2018; Hello and Fahad 2019). A variety of chloropropyl-modified MCM-41 silicas were synthesized by manipulating the TEOS to CPTES ratio in alkaline medium at 80 °C for generating catalytic active ionic liquids on its surface (Udayakumar et al. 2008). A number of physico-chemical measurements were used for analysis of obtained hybrid silicas. It was shown that the ordering of mesoporous structure decreased gradually with increasing of CPTES concentration in the synthesis gel. Nevertheless, co-condensation in combination with template applying allows producing silicas with larger and uniform pores, higher surface area, better long-range ordering, and well-distributed functionality in contrast to post-grafting technique. Wei et al. (2009) employed CPTES to functionalize ordered mesoporous silica (MCM-41 and MCM-48 silicas) through direct co-condensation (basic conditions, ambient temperature) and post-synthetic methods. The property function of the resulting composites was explored in detail to deeply understand the selective sorption of nitrosamines from aqueous solution. Surface and structure features of hybrid silicas were extensively characterized by X-ray diffraction analysis, nitrogen adsorption–desorption, ^{29}Si MAS NMR, ^{27}Al MAS NMR and TG-DSC together with FTIR technique. To examine the concentrations of functional silane influence on the modification process and the structure of final products, the molar percentage of CPTES varied between 1 and 15%. Also, a novel method of silica functionalization with CPTES was presented, where the surface-modified hybrid material was obtained from cheap waste product of the rice milling industry (Adam et al. 2009). This method involved a one-pot silica synthesis from sodium silicate and CPTES that does not require toxic reagents and proceeds within a reasonable time of 6 h without having to resort to high refluxing temperatures. A similar methodology was used for functionalization of silica with alkyl silane and organic ligands by Attol and Mihsen (2020), Hello et al. (2018), Hello and Fahad (2019), Sobh and Mihsen (2019). The optimum dosage of CPTES in the reaction mixture on the structure of chloropropyl-functionalized MCM-41 silica was also investigated for one-pot synthesis by the microwave radiation influence

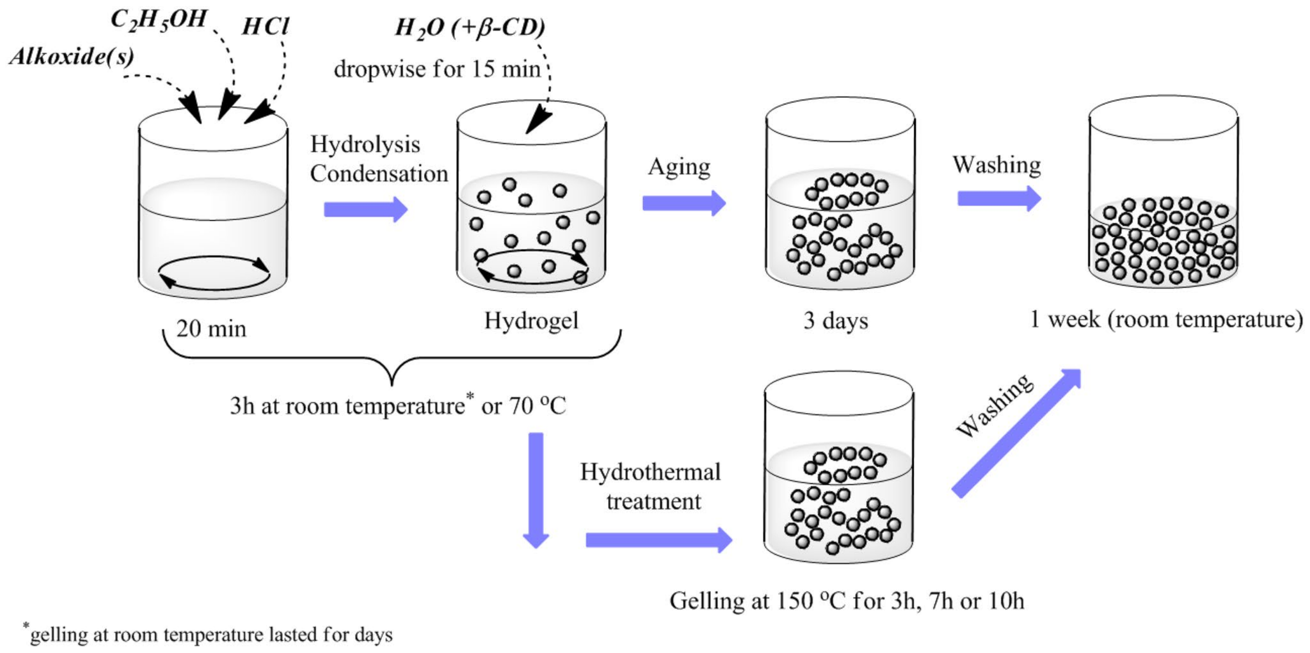

Scheme 1 The sequence of sol–gel silicas preparation procedure

(Xu et al. 2012). Single-factor analysis showed the optimal microwave power and time as well as dosage of CPTES for favorable formation of highly ordered MCM-41-$(CH_2)_3Cl$ mesostructure. Nevertheless, little is known about the influence of sol–gel synthesis conditions and functional silane dosage on the structure and composition of non-ordered silicas.

In this research, we report on the one-pot synthesis of hybrid silicas by co-condensation of TEOS and CPTES, systematically varying parameters of sol–gel reaction (molar ratios of initial silanes, temperature, time, and type of gel treatment). The effect of various synthesis conditions on the structure and properties of silicas was investigated by different physico-chemical methods of analysis (IR spectroscopy, chemical analysis of surface layer, SEM, low-temperature adsorption–desorption of nitrogen, and thermogravimetry). Moreover, we present attempts in preparing sol–gel silicas with covalently attached cyclodextrin moieties via a simple sol–gel technique, which does not require high temperature, toxic reagents and a huge investment of time due to the use of chloropropyl groups as anchoring centers for oligosaccharides immobilization. β-Cyclodextrin (β-CD) is cyclic oligosaccharide, which is torus-like macro-ring built up from seven glucopyranose units. The external part of β-CD molecule is hydrophilic, whereas the internal part is hydrophobic (Szejtli 1998). We used β-CD as complementary functional additive due to its complex-forming ability with many chemical substances (including toxic compounds) that may be useful in sorption processes. The probable effectiveness of hybrid silicas for toxic compounds removal from air and water was discussed. Gas-phase adsorption and liquid sorption experiments were carried out to study the role of silica structure and composition on benzene and phenol uptake, respectively.

Experimental section

Materials

Tetraethyl orthosilicate (TEOS) (≥ 99%, Merck) and (3-chloropropyl)triethoxysilane (CPTES) (≥ 95%, Aldrich) were used without additional purification. Supramolecular compound, β-cyclodextrin hydrate (β-CD) (99%, Acros Organics), was used as received (the water content was 11.7% according to the thermogravimetric analysis). Ethanol (96%) and hydrochloric acid (37%) were purchased from Reakhim. These reagents were of chemical grade and used without further purification. Benzene (pure analytical, Reakhim) and phenol (GR for analysis, Lachner) were used as purchased. Distilled water was used for all experiments.

Synthesis

Sol–gel silicas were synthesized via acidic hydrolysis (0.1 M HCl) of TEOS (alkoxysilane precursor with moderate reactivity) used solely or combined with CPTES (functional precursor) in different proportions (TEOS/CPTES molar ratio was 8:1, 5:1, 3:1, and 2:1, respectively) (Scheme 1). Ethanol was applied as solvent in constant molar concentration for all experiments. A solution of silica precursor or alkoxides' blend with catalyst and solvent was mixed on magnetic stirrer about 20 min. β-CD was put into reaction slurry to obtain hybrid silica with immobilized oligosaccharide moieties on its surface. The appropriate amount of water was added slowly throughout 15 min in each reaction vessel under continuous stirring to cause hydrolysis of the alkoxysilane compound(s). Since the water content is one of the most important factors for sol–gel reaction, which determines the hydrolysis rate, the molar ratio of H_2O to HCl was fixed at 10:0.3. Prepared reaction solutions were stirred vigorously until a clear solution was obtained. Temperature of reaction slurry and type of its treatment (hydrothermal treatment during different periods) were varied to find a correlation between the synthesis procedure conditions and the surface properties of obtained silicas. Gelling of sols was carried out at room temperature, when the total mixing of reaction blend on magnetic stirrer lasted for 3 h, and then obtained hydrogel was kept until the complete solidification has taken place. Also, gels were obtained at 70 °C until the viscosity of the solution was gradually increased and finally solidified into a jelly-like uniform mass. In addition, the gelling of sols was realized via hydrothermal treatment (HTT) in autoclave at 150 °C for 3 h, 7 h, and 10 h. For this purpose, TEOS (or TEOS/CPTES and β-CD)–ethanol–acid–water clear solution was transferred into quartz tube and inserted in stainless steel autoclave after agitating. All resulting solid gels were aged at room temperature for three days. Then they were washed on vacuum filter with distilled water for several times until the negative reaction for halogenide anions with $AgNO_3$. Also, the part of resulting gel from hydrolysis and condensation of TEOS and β-CD was not washed on vacuum filter, and just triplicate adding of 200 ml distilled water and following decantation was used (such samples of silicas were designated as "unwashed samples"). The solid products were dried at ambient temperature and then were kept in the desiccator.

In general, synthesized silicas were divided on four groups, which are different due to initials reagents of sol–gel reaction and synthesis conditions (Fig. 1). Sol–gel materials were labeled in terms of initial components, their molar composition and synthesis conditions. For example, the name of sample *TEOS_70* means that this silica was obtained from only one type of alkoxide at temperature 70 °C (without numbers were marked silicas obtained at ambient temperature (17–18 °C)); *TEOS/β-CD_150_3* corresponds to silica, synthesized from TEOS with β-CD additive and treated in autoclave at 150 °C during 3 h; the sample *TEOS/CPTES(8:1)_70* was prepared from the blend of two silanes with molar ratio 8:1 at temperature 70 °C, and its analog with oligosaccharide compound was named as *TEOS/CPTES/β-CD (8:1)_70*.

Analysis

IR spectroscopy was performed on Thermo Nicolet NEXUS FTIR spectrophotometer equipped with an environmental chamber for selector DRIFT. The spectra were obtained in the KBr mode, using KBr pellets with 1:20 ratio of silica sample and KBr, respectively. Infrared reflection spectra were registered in the range from 4000 to 400 cm^{-1} with resolution of 4 cm^{-1}. The experiments were conducted in air at room temperature.

Chemical analysis of surface oligosaccharide compounds was carried out by acid hydrolysis of cyclodextrin up to glucose and its subsequent spectrophotometric determination. The methodology of cyclodextrin content determination was described in detail in our previous works (Roik and Belyakova 2011; Trofymchuk et al. 2017). SEM analysis was performed on VEGA 3 SBU Tescan microscope.

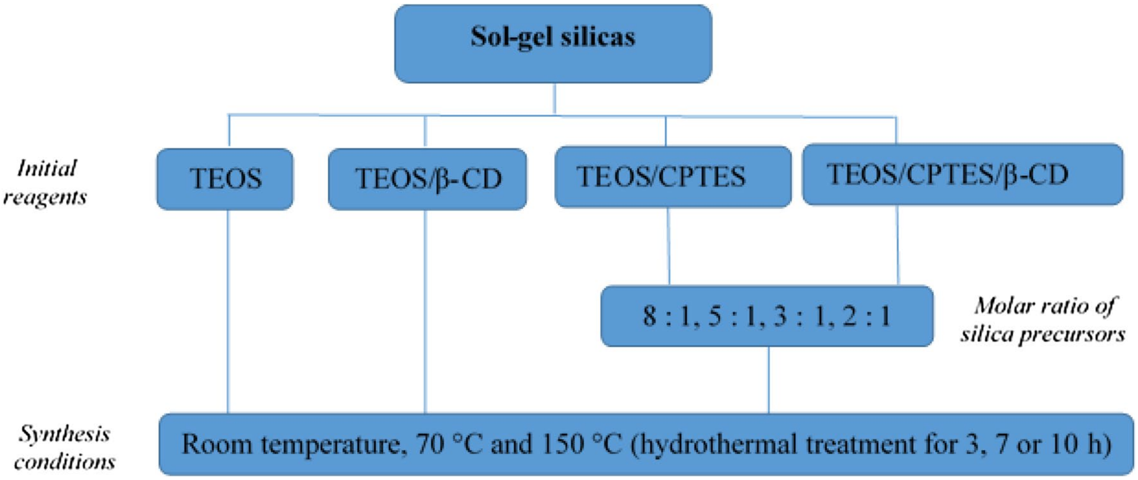

Fig. 1 Schematic diagrams of the sample preparation

Nitrogen adsorption–desorption isotherms were obtained on Nova 1200 apparatus from Quantachrome Corporation. Prior to the measurements, all silica samples were outgases under vacuum at 140 °C for 20 h. Specific surface areas were evaluated by Brunauer–Emmet–Teller (BET) method (Fagerlund 1973) and pore diameters were calculated by Barrett, Joyner, and Halenda (BJH) method (Barrett et al. 1951), based on the desorption branch of isotherms. The total pore volume was determined at $P/P_0 = 0.99$.

Thermogravimetric analysis was carried out on a Derivatograph-Q (MOM) in the temperature range 30–600 °C with a heating rate of 10° min^{-1} in air. The batch weight for sol–gel silicas was 20–30 mg. The quantity of immobilized organic groups was determined from TG curves.

Sorption experiments

Gas-phase adsorption of benzene

Adsorption of gaseous benzene was measured using McBain–Bakr gravimetric method (McBain and Bakr 1926) on a home-made laboratory apparatus equipped with a quartz spring balance at 25 °C. Quartz springs were calibrated before experiments. Spring elongations were monitored by cathetometer. The batch of silica samples used for these experiments was about 100 mg. All silicas were outgassed in a vacuum (a pumping system provided the vacuum $1.5\text{–}5 \cdot 10^{-2}$ mmHg) at 140 °C for 3 h prior to adsorption measurements. The saturation time was 1 h for each experimental point. The results of gas-phase adsorption were represented graphically by plotting the amount of adsorbed benzene versus the relative vapor pressure.

Liquid sorption of phenol

Multi-batch sorption tests were carried out to examine the efficiency of synthesized sol–gel silicas toward phenol uptakes from water at room temperature. In kinetic experiment, series of air-dried silica batches (0.1 g) were placed in stoppered glass vials (protected from sunlight) and 10 ml of 1 g/L phenol was added. The suspensions were stirred for predetermined time intervals, then the concentration of phenol in aliquots was determined by measuring the optical density with UV–Vis Specord M-40 spectrophotometer.

Adsorption isotherms were obtained by adding 0.1 g of air-dried silica sorbents to air-tight vials, and poured with aqueous solutions of phenol with predetermined concentration (from 0.1 to 1 g/L). After the adsorption equilibrium was reached, solutions were separated on paper filters.

Phenol concentration in each solution from kinetic and equilibrium experiments was analyzed by UV spectrophotometry at $\lambda = 270$ nm. The content of aromatic compound in filtrate was calculated from calibration curves. The amount of phenol sorbed on sol–gel silicas from water was evaluated as:

$$a = \frac{(C_0 - C_f)V}{m},$$

where a—sorption, mmol/g; C_0—initial concentration of aromatic compound in aqueous solution, mmol/L; C_f—concentration of aromatics in filtrate, mmol/L; V—volume of the aqueous solution of phenol, L; m—mass of adsorbent, g.

Results and discussion

Synthesis and characterization of sol–gel silicas

The sol–gel process gaining renewed interest because it provides a convenient way for incorporation, immobilization, entrapment, and encapsulation for a large variety of reagents including organic, inorganic, biomolecules, and macrocyclic compounds. The organic/inorganic hybrid materials made by this way are often characterized by unique combinations of properties, and the optimization of these properties can be achieved due to well-controlled composition of initial mixture at temperatures under the organic moieties can be unharmed.

As mentioned above, all silicas were prepared by acid catalyzed sol–gel mechanism. In acid conditions, hydrolysis is faster than condensation. The rate of condensation slows down with increasing number of siloxane linkages around a central silicon atom. This leads to weakly branched polymeric networks and promotes the development of more linear molecules in the initial stages of synthesis for all samples (Vansant et al. 1995). The next gelation step is influenced by many factors, among which the nature and concentration of structure forming components as well as temperature are crucial. The type and the size of the alkoxy group can strongly influence the hydrolysis and condensation reactions through a steric or leaving-group effect (Wen and Wilkes 1996). It was found that the gelation process of the *TEOS/CPTES* silicas was slower than that of *TEOS* itself. Besides, increasing amount of functional silane in alkoxide blend (TEOS/CPTES molar ratio from 8:1 to 2:1) leads to deceleration of gelation rate, which could directly affect the porous structure of the final product. This observation was confirmed in previously reported researches, when adding a very small amount of functional silane remarkably decreased the gelation time of TEOS acid solutions (Mah and Chung 1995; Wang et al. 2007). Also, applying β-CD as one of the reaction mixture components slows down even more the rate of gelation. For example, *TEOS* silica in the process of hydrolysis and condensation appeared homogeneous and then led to gel for two weeks at ambient temperature.

Addition of functional CPTES silane to the reaction mixture increases this time to several weeks. Furthermore, sol–gel solutions with oligosaccharide additives at room temperature undergo phase separation as a result of a significant gelation slowdown. Meanwhile, the rising of temperature in sol–gel process accelerates the gelling. Thus, homogeneous *TEOS/β-CD* and *TEOS/CPTES/β-CD* hydrogels were obtained in several hours when the temperature rises up to 70 °C. For reaction mixtures with both oligosaccharide compounds and organo-functional silane, the gel point was observed after continuous heating from 3 to 5 h for *TEOS/CPTES/β-CD(8:1)_70* and *TEOS/CPTES/β-CD(2:1)_70*, respectively. It is known that HTT is quite a simple procedure that is used for both varying the parameters of porous structure and more effective modification of silica surface (Leboda and Mendyk 1991). With the increase of temperature under hydrothermal conditions (at 150 °C), silica hydrosols underwent gelation for 3, 7 or 10 h. Despite that due to HTT usage we managed to get homogeneous hydrogels, the time processing of 3 h at 150 °C was not sufficient to obtain solid gel mass for all hydrosols. The gels of *TEOS/CPTES/β-CD(3:1)_150* and *TEOS/CPTES/β-CD(2:1)_150* silicas, for instance, were obtained under HTT during 4 and 7 h. Although prolonged HTT allows receiving stable gels, the result of TEOS and CPTES gelation with β-CD additive during more than 3 h obtained final products with color changed in comparison with other silicas (Fig. 2). Apparently, this effect can be explained by irreversible changes in the chemical structure of silica surface layer caused by beginning of organic moieties destruction.

Lastly, when gel is kept in contact with the pore-filling liquid (aging step), its structure and properties keep changing as a function of time. At drying stage, the changes in structure also occur. Therefore, the conditions at these two phases were constant for all synthesized silicas (except of silicas, obtained under HTT) (Scheme 1).

Depending on the composition of initial feedstock, it is possible to obtain hybrid silicas with different types of functional groups on the surface (Fig. 3). So for synthesized silicas, the structure is determined by siloxane group (≡Si–O–Si≡) with the oxygen atom on the surface and functional silanol groups (≡Si–OH) as a result of TEOS condensation (Fig. 3a); functional silanol as well as oligosaccharide groups on the surface, which could be

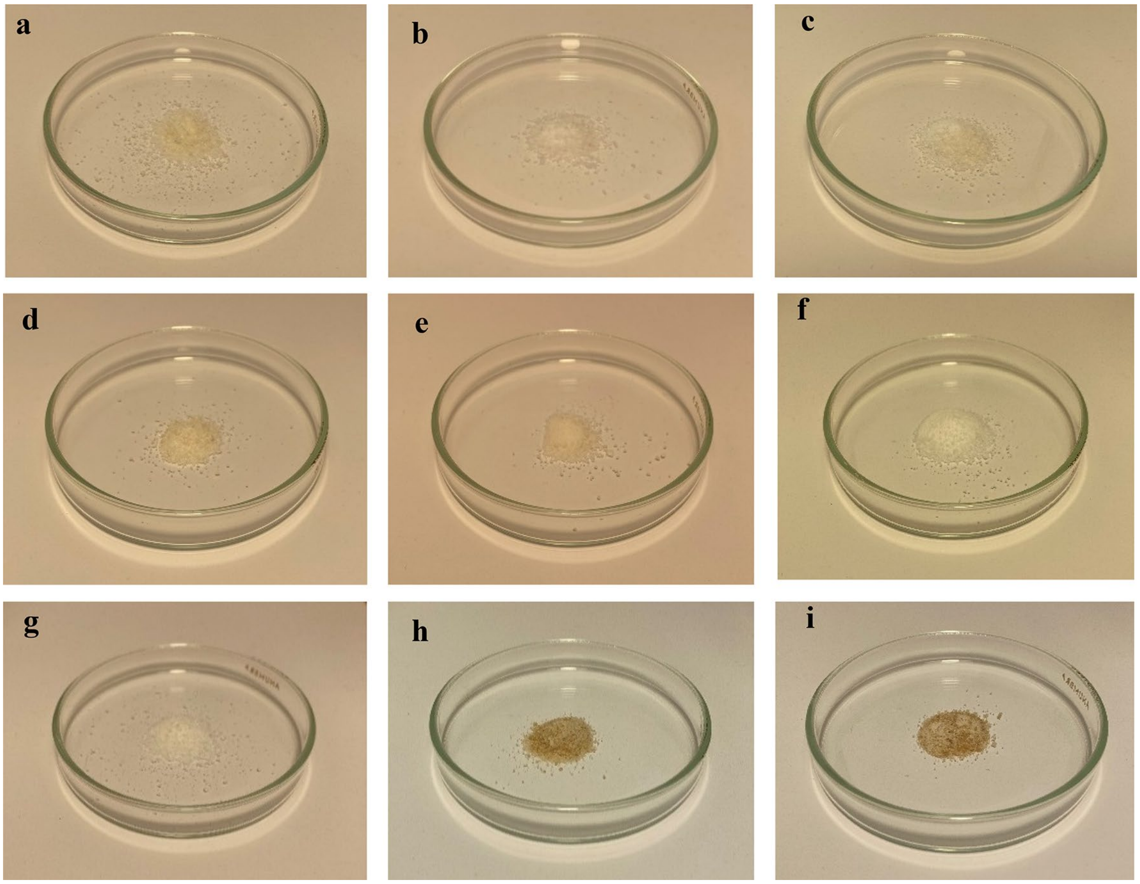

Fig. 2 Sol–gel silicas, obtained at different times of HTT (150 °C) from TEOS during 3 h (**a**), 7 h (**b**), and 10 h (**c**); TEOS/CPTES during 3 h (**d**), 7 h (**e**), and 10 h (**f**); and TEOS/CPTES/β-CD during 3 h (**g**), 7 h (**h**), and 10 h (**i**)

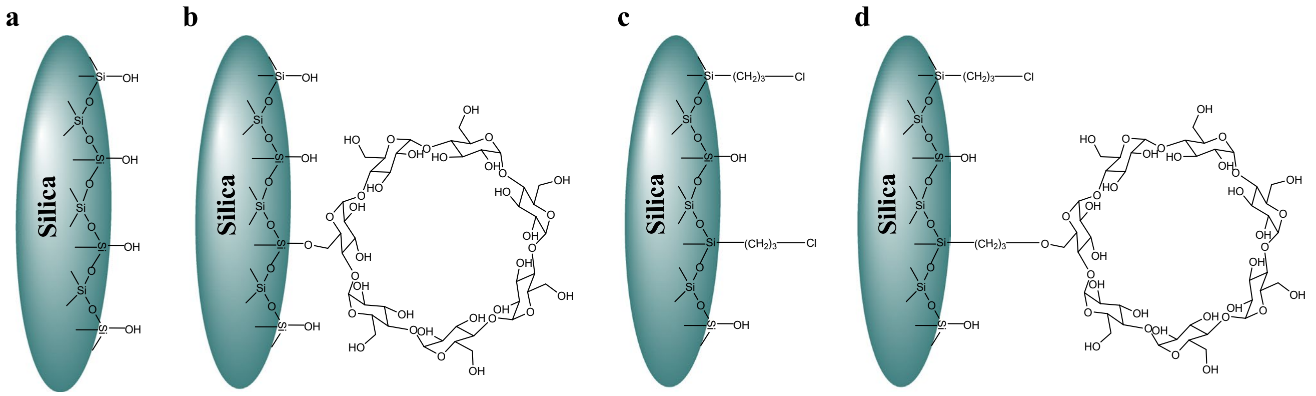

Fig. 3 Types of functional groups on the surface of synthesized silicas due to sol–gel hydrolysis and condensation of TEOS (**a**), TEOS with β-CD (**b**), mixed silane precursor TEOS/CPTES (**c**), and TEOS/CPTES with β-CD (**d**)

obtained using β-CD additive during TEOS condensation (Fig. 3b); functional silanol and 3-chloropropyl groups on the surface in consequence of TEOS/CPTES application (Fig. 3c); and all of the above-mentioned functional groups due to sol–gel hydrolysis and condensation of mixed silane precursors and supramolecule compound (Fig. 3d).

Chemical immobilization of functional groups on the surface of silica materials was proved by IR spectroscopy. There appear various IR vibrations of bands for different functional groups in the spectra of synthesized silicas (Table 1, Fig. 4). The silanol groups disposed on the silica surface and the presence of remaining water molecules produced the broad stretching band around 3046 cm^{-1}, followed by a band around 1640 cm^{-1}, attributed to bending vibration $\delta_{O\text{–}H}$. A strong absorption band near 1100 cm^{-1}, attributed to asymmetric stretching of Si–O–Si bonds, was observed in all silica samples.

It was shown that β-CD-containing silicas prepared from TEOS in water–ethanol solution with acid catalyst are hydrolytically unstable, and oligosaccharide moieties are attached to solid matrix presumably or mostly by forming Si–O–C linkages. However, the formation of hydrogen bonds between silanol groups of silica and hydroxyl groups of β-CD is possible too. In the IR spectrum of washed silica obtained from TEOS/β-CD mixture, there is no clear maximum in the range 3800–3150 cm^{-1} as in the spectra of β-CD and β-CD-containing xerogel, which is likely caused by the stretching vibrations of the O–H bonds in the hydroxyl groups of β-CD connected by hydrogen bonds (Fig. 5a). Also, the absorption band with maximum at 2932 cm^{-1} (stretching vibrations of the C–H bonds in the CH and CH_2

Table 1 Assignments of IR peaks (Bellamy 1975)

Peak position (cm^{-1})	Assignment of vibrations
3320	O–H stretching (β-CD)
3046	O–H stretching (silica silanols, water, β-CD)
2960	C–H stretching (chloropropyl silica)
2943	C–H stretching (β-CD silica)
2932	C–H stretching (CH and CH_2 groups of β-CD)
2930	C–H stretching (β-CD)
1640	H–O–H bending (silicas, water, β-CD)
1400–1200 (1443, 1356, 1310, 1273), 1200–900	C–H bending; C–O, C–OH, and C–O–C stretching (β-CD, chloropropyl silica, β-CD silica)
1400–1200	ν(C–O) and δ(C–H)
1200–1030 (1078, 1030)	C–O stretching (ether and hydroxyl groups of β-CD)
1100–1000	Si–O–Si and Si–O–C stretching
960	Si–O(H) stretching
950–700	C–H bending and pulsation (glucopyranose cycle)
690	C–Cl stretching vibration
500–400	Si–O–Si bending vibration

Fig. 4 IR spectra of β-CD (**a**) and silicas prepared at 70 °C from TEOS (**b**), TEOS/CPTES (**c**), and TEOS/CPTES/β-CD with molar ratio of silanes 5:1 (**d**). On the right, scaled-up inserts of spectra in the range 3200–2700 cm^{-1} and 1500–1000 cm^{-1}

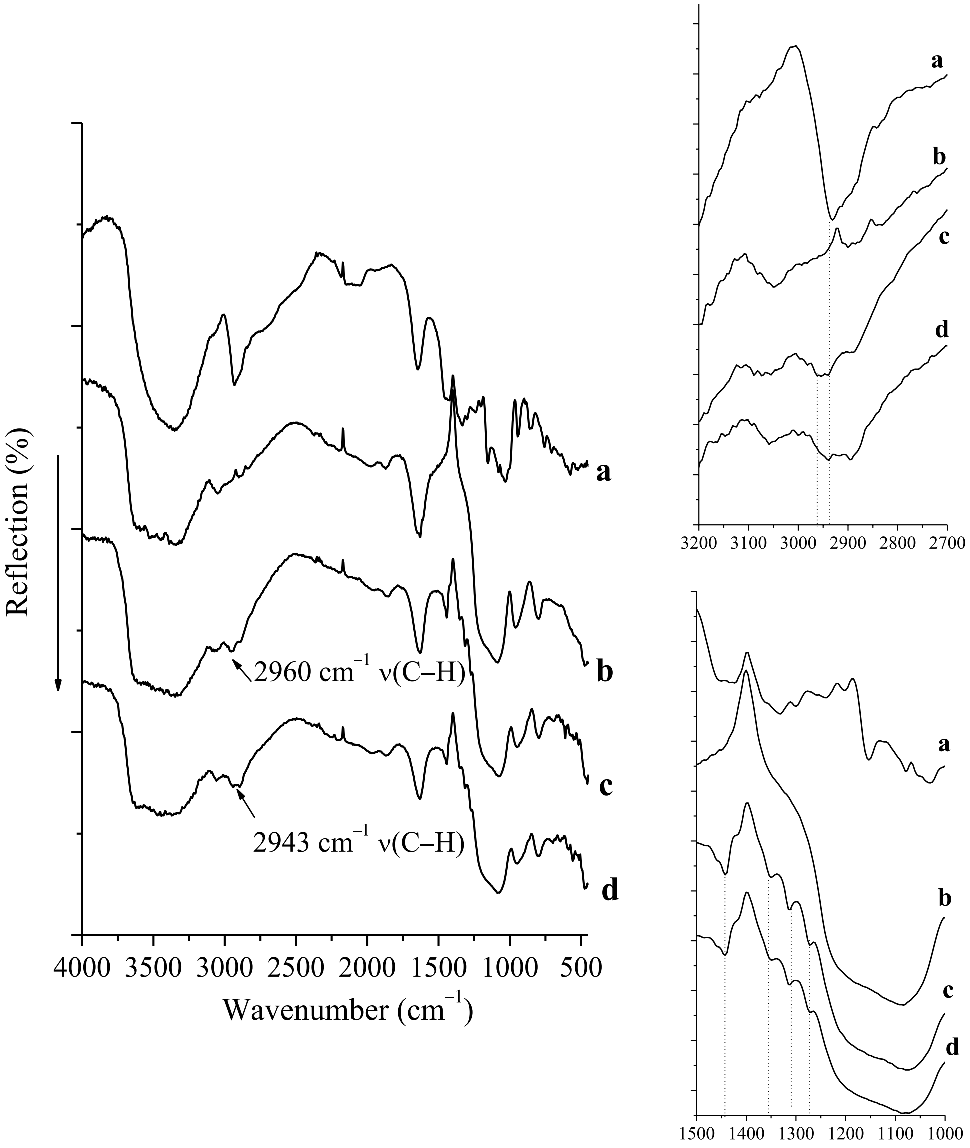

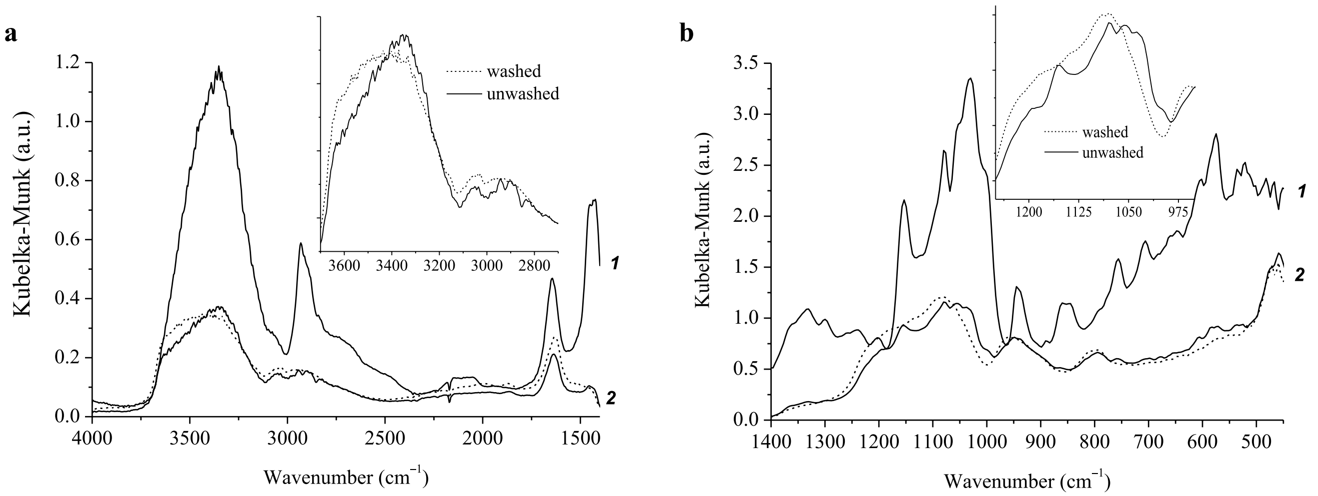

Fig. 5 IR spectra of β-CD (curve *1*) and β-CD-containing xerogel (curve *2*) prepared from TEOS at 70 °C (dashed line refer to spectrum of washed sample) in the regions 4000–1400 cm^{-1} (**a**) and 1400–450 cm^{-}.^{1} (**b**)

groups of β-CD molecules) disappears in washed xerogel. The band assignments in the IR spectra of β-CD and β-CD-containing xerogel in the interval 1400–500 cm^{-1} showed that absorption bands of β-CD groups were present only in unwashed xerogel (Fig. 5b). Thus, the absorption bands of the bending vibrations δ_{C-H} in the primary and secondary hydroxyl groups of β-CD are registered in the region 1400–1200 cm^{-1}. In the interval 1200–1030 cm^{-1}, the absorption bands of the stretching vibrations of the C–O bonds in the ether and hydroxyl groups of β-CD (1078 and 1030 cm^{-1}) are observed. The Si–O–C bond gives rise to intense bands in the region 1100–1000 cm^{-1} due to the antisymmetric stretching mode. For washed silica, these bands are shifted and decreased in intensity. The absorption bands in the range 950–700 cm^{-1} belong to bending vibration δ_{C-H} and the pulsation vibrations in the glucopyranose cycle.

The drastic decrease of β-CD moieties on the surface of β-CD/TEOS material (after washing) was also confirmed by chemical analysis (Table 2). As can be seen, the quantity of oligosaccharide immobilized on sol–gel silica after hydrolysis and condensation of TEOS with β-CD at 70 °C decreases from 117.55 μmol/g to 2.68 μmol/g after repeated rinsing with water.

Hydrolytically stable CD-containing silicas could be prepared by hydrolysis and condensation of TEOS and CPTES. In the presence of CPTES, stronger C–O–C linkages are possible to form. IR spectra of pristine silica, functionalized organosilica with chloropropyl groups and CD-containing silica are shown in Fig. 4b–d. In the IR spectra of organosilica materials, absorption band of bending vibrations of the C–H bonds at 1443 cm^{-1} is observed. After the hydrolysis and polycondensation of TEOS/CPTES mixture both in the absence and presence of β-CD, the characteristic bands in the region 1400–1200 cm^{-1} and 1200–900 cm^{-1} appeared in the spectra of silica materials. These bands are related to the valence vibrations of the C–O, C–OH, and C–O–C bonds as well as deformation vibrations of the C–H bonds. Indication of the presence of CDs on silica surface is the appearance of specific vibration band ascribed to β-CD at 2943 cm^{-1}. A band at 690 cm^{-1} can be assigned to stretching vibration of C–Cl bond. Table 1 lists the analyzed IR absorption peaks of synthesized silicas.

Table 2 Elemental analysis of particles' surface by SEM for synthesized sol–gel silicas

Silica	Element (mass %)			
	Si	O	C	Cl
TEOS	25.7	40.34	–	–
TEOS/β-CD_70 (unwashed)	27.6	50.8	21.3	–
TEOS/β-CD_70	31.5	41.2	3.8	–
TEOS/CPTES(5: 1)_70	26.6	32.8	8.3	5.0
TEOS/CPTES/β-CD(5: 1)_70	29.6	36.9	9.3	4.7

The band assignments in IR spectra as well as chemical analysis confirm the presence of β-CD on the surface of synthesized materials. Since the primary hydroxyl groups of the β-CD are more nucleophilic, more basic and less sterically hindered than the secondary hydroxyls, they exhibit greater reactivity. Consequently, β-CD is predominantly attached via these groups on an appropriate spacer to the surface (Lubda et al. 2003). However, the formation of Si–O–C or C–O–C bounds with participation of the secondary hydroxyl groups of β-CD is not excluded.

Quantitative chemical analysis was performed for several types of sol–gel organosilicas with attached oligosaccharide moieties. The results are represented in Table 2. As mentioned above, hydrolytically unstable Si–O–C linkages are formed as a result of sol–gel synthesis of CD-containing silicas from TEOS with β-CD additive. The content of cyclic macromolecules on the surface layer of unwashed *TEOS/β-CD_70* and *TEOS/β-CD_150_3* silicas consists of 117.55 and 111.96 μmol/g correspondingly, whereas these values are reduced by two orders of magnitude (2.68 and 2.30 μmol/g, respectively) after multiple washing of silicas with water. Evidently, that silica prepared from sol–gel hydrolysis and condensation of TEOS in the oligosaccharide presence is unlikely to be used as a sorbent for the removal of toxic contaminants from water. At the same time, β-CD immobilized through CPTES anchoring centers is removed from the surface of synthesized sol–gel silicas only by acid hydrolysis. Moreover, chemical analysis data show more effective immobilization of oligosaccharides moieties with increasing TEOS: CPTES ratio. *TEOS/CPTES/β-CD(8:1)_70*, *TEOS/CPTES/β-CD(5:1)_70*, and *TEOS/CPTES/β-CD(3:1)_70* silicas contain 3.54, 4.83, and 4.94 μmol/g of covalently attached β-CD, respectively. Hence, the obtained results indicate that stronger C–O–C linkages are formed as a result of TEOS/CPTES blend co-condensation with β-CD. Unexpectedly, the increase in hydrothermal temperature did not result in any enhancement of immobilized oligosaccharide on the surface of sol–gel silica in comparison with materials prepared at 70 °C. Although synthesized CD-containing sol–gel silicas with C–O–C linkages show moderate oligosaccharide groups loadings, they are hydrolytically stable and can therefore be considered for the sorbents preparation (by simple time-saving method) for removal of toxic compounds from aqueous medium. Also it should be noted that the content of immobilized organic groups on the surface is usually less than expected for the most of research works on silica sol–gel synthesis. Hoffmann et al. (2006) pointed that the quantity of organic functionalities in the modified silica phases does not normally exceed 40 mol%. Furthermore, it was denoted that concentration of incorporated terminal groups on the pore-wall network is generally lower than their concentration in the initial reaction mixture. The reason for reducing content of incorporated functional groups is most likely an increase in the number of homocondensation reactions in reaction slurry with certain alkoxysilanes ratio due to crosslinking co-condensation reactions with the silica precursors. Moreover, if considered such hybrid silicas as promising sorbents for water purification, then not only the quantity of immobilized functional groups, but also the porous structure of materials plays an important role.

The morphological characteristics of synthesized sol–gel silicas were evaluated by SEM analysis. Figures 6 and 7 display SEM images of synthesized silicas photographed under various magnifications. As shown by SEM images (Fig. 6), *TEOS*, *TEOS/CPTES*, and *TEOS/CPTES/β-CD* materials reveal a similar morphology of irregular rock-like particles with smooth surface. Compared with *TEOS* (uniform particles; size no more than 1 mm), hybrid silicas possess amorphous particles with diverse size. Moreover, the particles' surface of silicas obtained with oligosaccharide additives found to be rough with small holes spread among rocky pieces. Figure 7 shows SEM images of TEOS silica prepared with β-CD before and after multiple rinsing with water. As can be seen, on the surface of *TEOS/β-CD_70* (unwashed) particles, there are certain formations, and their shape and size correspond to agglomerates of β-CD mentioned in other studies with SEM analysis applied (Rajbanshi et al. 2018). After washing, a surface of particles becomes smooth, and similar surface defects are visible for TEOS/β-CD as in the case of TEOS/CPTES/β-CD particles at high magnification. It is obvious that oligosaccharide as component of reaction slurry has certain influence on the structure of sol–gel silicas.

Elemental analysis obtained with SEM correlates well with chemical analysis (Table 3). Although it does not show stoichiometric relationship between silica and surface immobilized groups, the presence of increased amounts of C (more than 20%) for unwashed *TEOS/β-CD* in comparison with multiple rinsed ones proves that hydrolytically stable chemical linkages are not formed because of sol–gel synthesis from TEOS with β-CD additive. At the same time, the existence of Cl in elemental analysis for *TEOS/CPTES* and *TEOS/CPTES/β-CD* silicas is a strong evidence, indicating the successful incorporation of 3-chloropropyl groups into the silica matrix. A slight decrease in mass % of Cl and an increase in mass % of C and O in elemental analysis of *TEOS/CPTES/β-CD* silica particles may indicate the attaching of β-CD groups on the silica surface.

The effect of synthesis conditions, oligosaccharide additive, and functional silane on structure of resulting silicas was estimated by low-temperature nitrogen adsorption–desorption. A similar shape of isotherms is observed for all series of synthesized silica. Figure 8 shows a typical form of isotherms for sol–gel silicas prepared by hydrolysis and condensation of TEOS itself, TEOS/CPTES mixture, and TEOS/CPTES with β-CD. Here, it should be noted that the shape of isotherm for *TEOS/β-CD* silica (unwashed) is analogous to isotherm of functionalized sample (but with extended hysteresis loop), and after multiple washing of this silica material, the form of isotherm becomes identical to *TEOS* silica ones. According to the common classification of adsorption isotherms, the isotherms for all synthesized silicas are considered as Type I (Sing 1989). Thommes et al. (2015) proposed updated classification of physisorption isotherms, pursuant to which isotherms of synthesized sol–gel silicas display Type I(b). In general, reversible Type I isotherms are characteristics of microporous solids with relatively small external surfaces, for example some activated carbons, molecular sieve zeolites and certain porous oxide. For materials with a large number of micropores, a steep uptake at very low P/P_0 on isotherms is observed that could be caused by enhanced adsorbent–adsorptive interactions in narrow holes. According to Thommes et al. (2015), Type I(b) isotherms are found in materials having pore size distributions over a broader range including wider micropores and possibly narrow mesopores ($<\sim$ 2.5 nm).

It could be concluded that there are no drastic changes in the morphology of materials after modification with chloropropyl and cyclodextrin moieties. However, isotherms of silica prepared from TEOS/CPTES mixture and β-CD silica composites shifted to lower total volume and exhibited narrow hysteresis loops in the wide range of P/P_0. This hysteresis (H4 type) is not seen in the isotherm of pristine silica prepared from TEOS. The appearance of such hysteresis loops could be explained by the presence both micro- and mesopores (Thommes 2010; Thommes et al. 2015). The pore size distribution estimated from the desorption branch of the isotherm is narrower for pristine silica and CD silica composite with the average pore diameter near 2.5 nm.

Specific surface area, pore volume, and pore size distribution are requisite parameters for physical characterization of the silica surface. These properties are critical in many application fields, especially in catalysis and separation. Structural parameters of synthesized sol–gel silicas were determined from low-temperature nitrogen adsorption–desorption isotherms and summarized in Table 2.

The specific surface area S_{BET} of pristine silica, synthesized from TEOS at ambient temperature, is very high (874 m^2/g). Clearly, increasing the temperature of synthesis altered the textural characteristic of materials. Thus, S_{BET} and mesopore volume V_{meso} for *TEOS_70* silica are almost the same as for *TEOS* silica, whereas micropore volume V_{micro} greatly reduces from 0.11 to 0.03 cm^3/g. Rise in temperature to 150 °C leads to changes in structural parameters of sol–gel silicas. It is observed as the decrease of S_{BET}, V_{meso}, and total pore volume V_t for materials prepared under

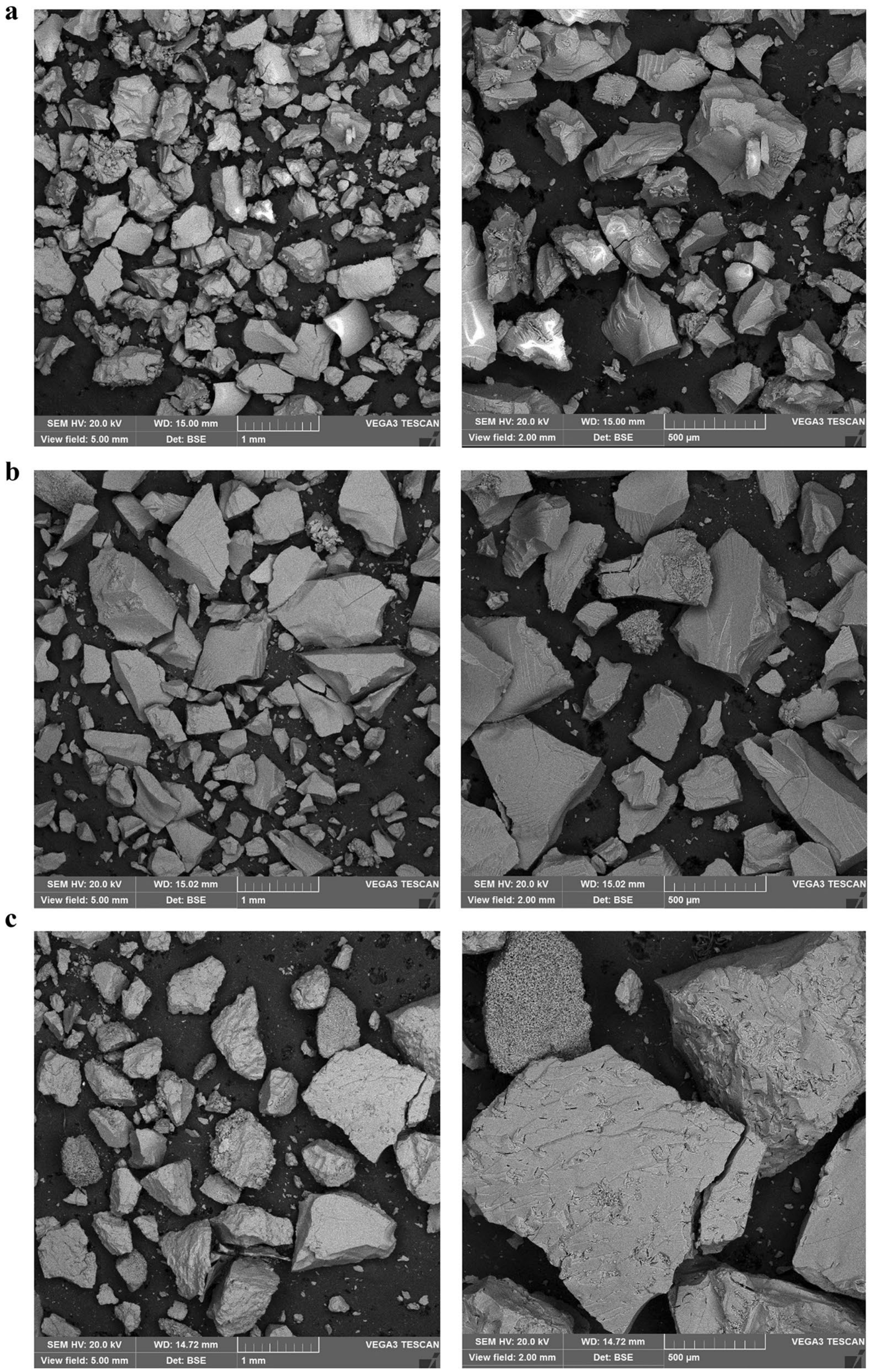

Fig. 6 SEM images of sol–gel silicas prepared from TEOS (**a**), TEOS/CPTES (**b**), and TEOS/CPTES/β-CD (**c**) at 70 °C

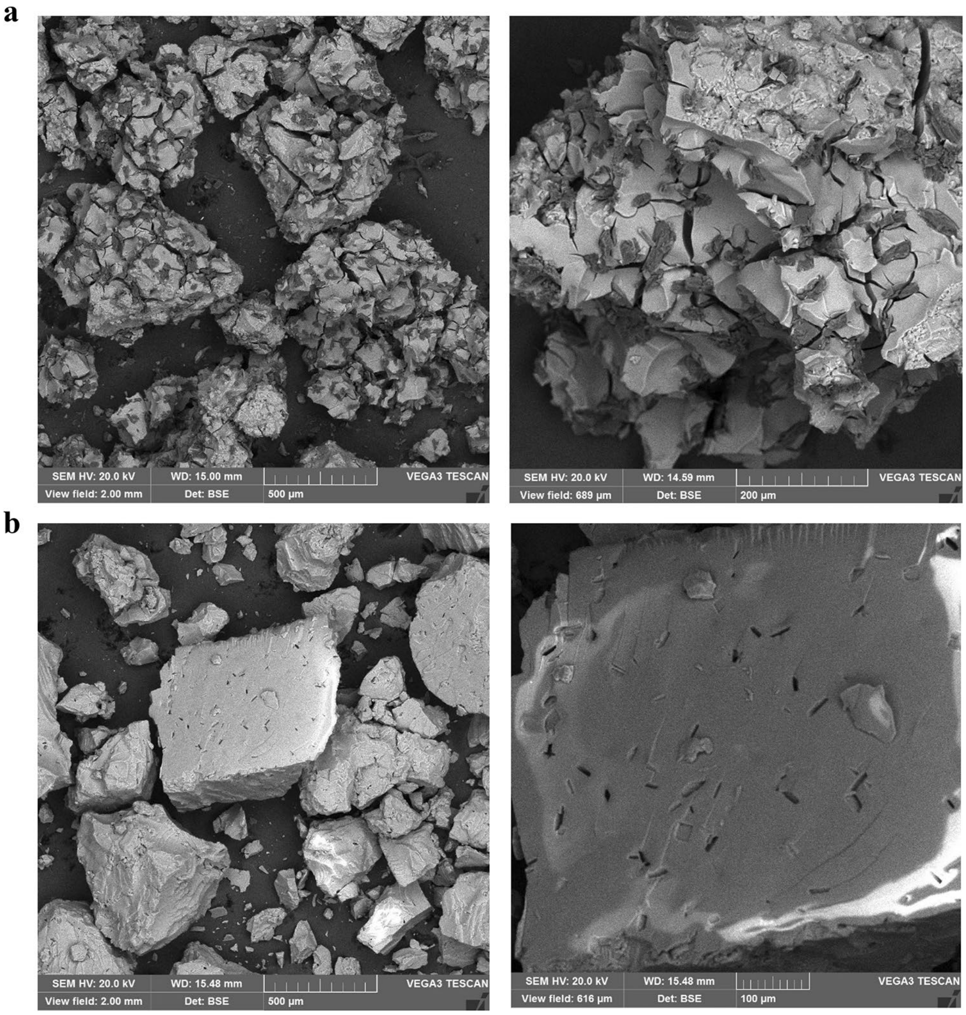

Fig. 7 SEM images of sol–gel silicas prepared from TEOS and β-CD at 70 °C before (**a**) and after (**b**) multiple washing

HTT. The reduction of specific surface area for samples prepared under HTT conditions can be explained by Oswald ripening processes (Voorhees 1985). However, an increase in specific surface area was observed after submitting sol from 3 to 10 h at 150 °C under HTT.

Surface area and total pore volume decreased because of silica functionalization. It was expected since the occupation of a volume inside the pore space by bonded alkyl phase and oligosaccharide moieties. Such observations described elsewhere (Wei et al. 2009; Xu et al. 2012). At the same time, the total volume of micropores obtained from BJH model increases in the issue of silica functionalization. Interestingly, the addition of oligosaccharide during hydrolysis and condensation of TEOS causes the most noticeable changes in the values of S_{BET}, in particular for unwashed *TEOS/β-CD_70* silica. It is assumed that entrances of pores are blocked by cyclodextrin moieties. Obviously, after multiple washing, the apparent increase in specific surface area of *TEOS/β-CD_70* silica is associated with the formation of more open structure, which becomes accessible to nitrogen molecules. Besides, the increase of V_{micro} by an order of magnitude in multiple washed silicas could be explained by the role of cyclodextrin as template molecules during sol–gel process. This statement could also be supported by images of SEM analysis (Fig. 7b), where changes in particles' surface are clearly shown after silica rinsing.

As was mentioned above, the covalent modification of silicas with 3-chloropropyl moieties was also accompanied by decrease in S_{BET}, V_{meso} and V_t. The values of structural parameters are affected by the amount of silane used in the initial synthetic mixture. It should be noted that the variation of TEOS/CPTES molar ratio from 8:1 to 5:1 did not lead to drastic changes in the textural characteristic, whereas when the molar ratio in the initial mixture was equal to 3:1 and 2:1, specific surface areas and pore volumes considerably decreased. The addition of β-CD during co-condensation of TEOS/CPTES blend does not change significantly the structural parameters of obtained silicas. As can be seen from the Table 2, for *TEOS/CPTES/β-CD(8:1)_70* and *TEOS/CPTES/β-CD(5:1)_70* silicas, the values of S_{BET} are in the range 430–601 m^2/g and pore volumes are V_{micro} ~ 0.1 cm^3/g, V_{meso} ~ 0.2 cm^3/g, and V_{total} ~ 0.3 cm^3/g. These small

Table 3 Structural properties of sol–gel silicas

Silicas	CD-containing silicas									
	S_{BET} (m^2/g)	V_{micro} (cm^3/g)	V_{meso} (cm^3/g)	V_t (cm^3/g)	D (A)	S_{BET} (m^2/g)	V_{micro} (cm^3/g)	V_{meso} (cm^3/g)	V_t (cm^3/g)	D (A)	CD content (µmol/g)
TEOS	874	0.11	0.28	0.45	25.5	–	–	–	–	–	–
TEOS_70	863	0.03	0.29	0.49	25.3	48 (384)[a]	0.015 (0.12)[a]	0.003 (0.06)[a]	0.03 (0.25)[a]	33.3 (34.1)[a]	117.55 (2.68)[a]
TEOS_150_3	720	0.04	0.22	0.39	25.3	502	0.13	0.18	0.23	22.8	111.96 (2.30)[a]
TEOS_150_7	725	0.06	0.23	0.38	22.9	370	0.05	0.10	0.18	23.3	–
TEOS_150_10	752	0.06	0.25	0.40	23.0	386	0.04	0.13	0.18	25.0	–
TEOS/CPTES(8:1)	510	0.12	0.21	0.25	23.3	–	–	–	–	–	–
TEOS/CPTES(8:1)_70	530	0.13	0.20	0.26	21.9	533	0.13	0.20	0.25	22.3	3.54
TEOS/CPTES(8:1)_150_3	489	0.12	0.19	0.24	23.1	577	0.13	0.13	0.27	24.1	2.76
TEOS/CPTES(8:1)_150_7	592	0.07	0.16	0.30	22.9	583	0.10	0.14	0.27	23.4	–
TEOS/CPTES(8:1)_150_10	609	0.08	0.18	0.31	23.1	601	0.10	0.15	0.29	23.7	–
TEOS/CPTES(5:1)	512	0.09	0.14	0.27	25.8	–	–	–	–	–	–
TEOS/CPTES(5:1)_70	396	0.08	0.17	0.21	23.1	429	0.11	0.18	0.21	23.8	4.83
TEOS/CPTES(5:1)_150_3	470	0.08	0.16	0.25	26.7	485	0.08	0.13	0.24	24.7	2.66
TEOS/CPTES(5:1)_150_7	538	0.09	0.12	0.26	22.8	–	–	–	–	–	–
TEOS/CPTES(5:1)_150_10	589	0.07	0.16	0.30	22.7	–	–	–	–	–	–
TEOS/CPTES(3:1)_70	3.4	–	–	0.01	45.1	1	–	–	–	–	4.94
TEOS/CPTES(3:1)_150	481	0.07	0.15	0.26	25.2	458	0.06	0.12	0.22	23.1	–
TEOS/CPTES(2:1)_70	10	–	–	–	49.8	4	–	–	–	46.3	–
TEOS/CPTES(2:1)_150	15.6	–	0.02	0.02	42.0	–	–	–	–	–	–

[a] Multiple washed silica

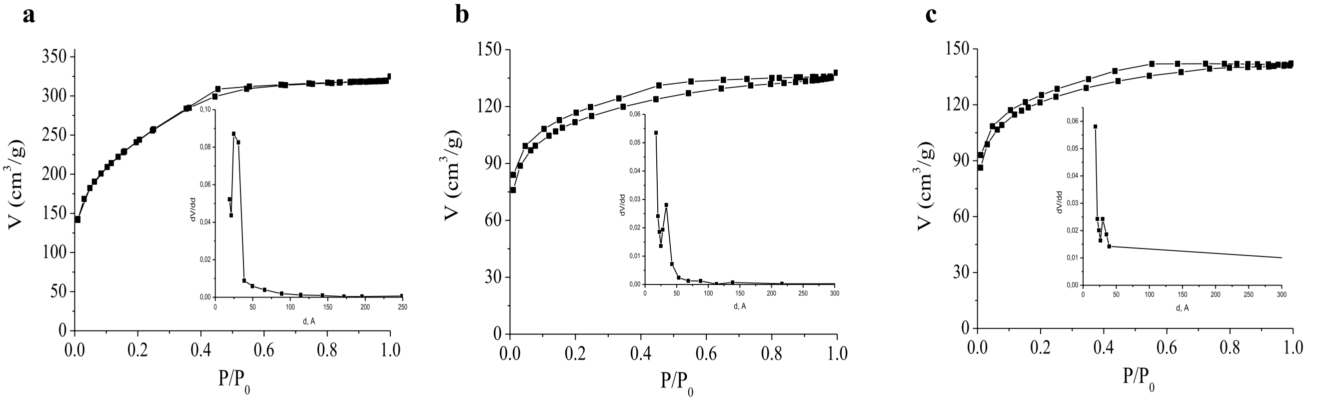

Fig. 8 Nitrogen adsorption–desorption isotherms and pore size distributions for silicas prepared from TEOS (**a**), TEOS/CPTES (**b**), and TEOS/CPTES/β-CD (**c**) at 70 °C

changes might indicate the low functionalization of silicas with oligosaccharide molecules in mild sol–gel synthesis conditions, which is also confirmed by chemical analysis. Moreover, for 3:1 and 2:1 TEOS/CPTES molar ratio, there is no considerable increase in the content of covalently attached β-CD according to the results of quantitative chemical analysis, but at the same time, these silicas become practically nonporous. The increased value of S_{BET} and the pore volumes for *TEOS/CPTES(3:1)_150* and *TEOS/CPTES/β-CD(3:1)_150* silicas have no clear explanation.

To determine the thermal stability of sol–gel silicas, thermogravimetric analysis was performed. Three series of samples (silicas from TEOS, silicas from TEOS/CPTES mixture, and β-CD silicas from TEOS/CPTES mixture) in our study have different thermo-destructions. Generally, it could be distinguished as two main regions in thermogravimetric curves with thermal events for all silicas. The region up to 150 °C corresponds to desorption of physically adsorbed water or perhaps residual solvent. The principal weight loss is observed in the region after 150 °C and related to the removal of organics accompanied by polymerization, structural relaxation, and bond shrinkage.

Figure 9 shows the typical results of thermal analysis for sol–gel silicas of three experimental series (in particular, TEOS_*70*, *TEOS/CPTES(8:1)*_70, and *TEOS/CPTES/β-CD(8:1)_70* silicas). The thermal events for

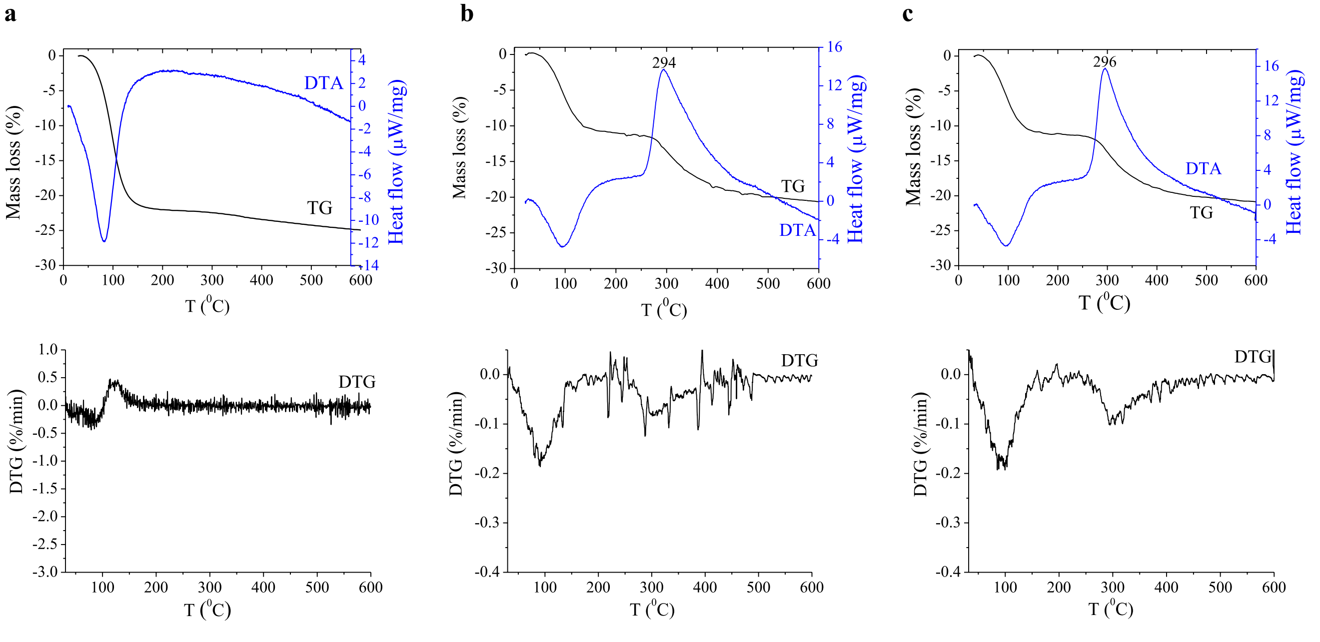

Fig. 9 Thermal analysis for silicas prepared from TEOS (**a**), TEOS/CPTES (**b**), and TEOS/CPTES/β-CD (**c**) at 70 °C

certain silica materials are compiled in Table 4. For the silica, prepared by hydrolytic condensation of TEOS, desorption of adsorbed water on the surface is observed when the temperature is about 100 °C (intensive weight loss corresponds to ~ 25%). When the temperature increases above 100 °C, the weight loss is caused by the water which is in pores. Then, the slow structure reorganization occurs without any noticeable peaks of mass loss. However, thermal behavior of silicas changes for TEOS/CPTES materials. Since organo-silane such as CPTES is likely to be more hydrophobic than TEOS, it follows that sol–gel silicas synthesized from TEOS/CPTES mixture may be preferentially more hydrophobic. The weight loss under 150 °C for chloropropyl-modified sol–gel silicas is small (6–9%) in comparison with pristine TEOS, because hydrophobic functional fragments prevent water adsorption. Noticeably, that the relative mass loss in the region up to 150 °C decreases, when the molar ratio TEOS/CPTES is changed from 8:1 to 5:1. These results indicate that the higher the concentration of CPTES in the initial sols, the lesser are the incorporated residuals such as water or solvent (ethanol). Also, organosilicas have more drastic weight loss at temperature above 300 °C, corresponding to the decomposition of chloropropyl fragments from the surface of modified silicas. There are exothermic peaks at 294 °C and 278 °C on DTA curves of *TEOS/CPTES(8:1)*_70 and *TEOS/CPTES(5: 1)*_70 silicas, confirming successful functionalization of silicas. Also, DTG curve exhibits many degradation shoulder peaks, indicating that the degradation mechanism of sol–gel silica containing chloropropyl groups is much complicated. The tendency of greater weight loss (from ~ 7% to 11%) in the second temperature region enhances with increasing CPTES concentration.

According to the thermogravimetric results obtained on β-CD silica materials, at the temperature 280 and 296 °C, the rate of weight loss was the most significant. This weight loss correlates with the thermal degradation of CD moieties on silica surfaces (Ponchel et al. 2004; Roik et al. 2017). It is worth noting that the loss of physically adsorbed water slightly increases for *TEOS/CPTES/β-CD(8:1)_70* and *TEOS/CPTES/β-CD(5:1)_70* silicas. It could be an additional confirmation of oligosaccharide moieties immobilization by sol–gel synthesis since the external surface of its molecules is considered hydrophilic. However, the appearance of the most intense thermo-effects in the same region for chloropropyl and cyclodextrin moieties as well as moderate quantity of immobilized organic groups by one-pot sol–gel synthesis does not allow the quantitative calculation of oligosaccharide content by the use of thermogravimetric analysis data.

Conclusively, based on the detailed analyses of synthesized sol–gel silicas, four samples of prepared materials were selected for further investigation, including the study of sorption properties toward aromatics in gas and liquid phases: *TEOS_70*, *TEOS/β-CD_70* (washed), *TEOS/CPTES(5:1)_70*, and *TEOS/CPTES(5:1)/β-CD_70*.

Sorption study

Silica porous materials with large specific surface area are of great importance as effective sorbents for the removal of different hazardous contaminants from air and water medium. In particular, they can be used for sorption of benzene and its derivatives, which are common organic compounds in industrial processes as well as daily human consumption and may contribute to serious environmental or human

Table 4 TG–DTA data of sol–gel silicas

Silica	Event	Temperature range (°C)	Weight loss (%)	DTA (°C)	Assignment
TEOS_70	I	30–150	25.3	102 (endo)	Dehydration (physically adsorbed water, residual solvent)
	II	150–600		–	Structure reorganization (condensation of the silanol groups)
TEOS/CPTES(8:1)_70	I	30–150	9.30	94 (endo)	Dehydration (physically adsorbed water, residual solvent)
	II	150–600	6.60	294 (exo)	Loss of chloropropyl chain, condensation of the silanol groups
TEOS/CPTES/β-CD(8:1)_70	I	30–150	9.48	96 (endo)	Dehydration (physically adsorbed water, residual solvent)
	II	150–600	6.97	296 (exo)	Loss of organics, polymerization, structural relaxation, bond shrinkage
TEOS/CPTES(5:1)_70	I	30–150	6.17	85 (endo)	Dehydration (physically adsorbed water, residual solvent)
	II	150–600	11.02	278 (exo)	Loss of chloropropyl chain, condensation of the silanol groups
TEOS/CPTES/β-CD(5:1)_70	I	30–150	7.06	87 (endo)	Dehydration (physically adsorbed water, residual solvent)
	II	150–600	10.98	280 (exo)	Loss of organics, polymerization, structural relaxation, bond shrinkage

health problems. It is recognized that hydrophobic hole of β-CD can act as a cage for the aromatic ring. Earlier (Guo et al. 1998; Kfoury et al. 2018; Landy et al. 2000; Szaniszlo et al. 2005; Trofymchuk et al. 2011), the formation of "host–guest" inclusion complexes between aromatics and cyclic oligosaccharide was confirmed. The idea of present research was to use both complexation ability of β-CD and excellent properties of silica as sorbent for chemical tailoring of new materials, and to investigate their sorption interaction with benzene and phenol as model pollutants.

Silica material *TEOS/CPTES/β-CD(5:1)_70* with developed porosity and content of surface oligosaccharide groups equal to 4.83 μmol/g was adopted here as a representative sample to estimate benzene gas-phase adsorption and phenol removal from aqueous medium, comparing with pristine and chloropropyl-functionalized silicas. Also, sorption studies were conducted for *TEOS/β-CD* silica (multiple washed) prepared by hydrolysis and condensation of TEOS in the presence of cyclic oligosaccharide (residual amount of β-CD equal to 2.68 μmol/g) because of its different values of textural parameters as compared to above-mentioned silicas.

An amount of benzene adsorbed at various pressures on synthesized silica materials was measured with a McBain–Bakr balance by noting the extension of a quartz spring due to the increase in sorbent weight. The static benzene adsorption isotherms on silica samples are presented in Fig. 10.

In the first and the lowest pressure region ($0 < P/P_S < 0.2$), three types of synthesized materials (*TEOS/β-CD_70*, *TEOS/CPTES(5:1)_70*, and *TEOS/CPTES/β-CD(5:1)_70* silicas) exhibited similar behavior with sharp increase in benzene equilibrium adsorption, suggesting their high affinity to aromatic compound. Contrary, pristine *TEOS_70* showed lower benzene uptake at the initial stage. Obtained result can be explained by dependence of benzene adsorption on micropore volume of silica material, since the closely spaced pore walls enhance the physical adsorption (Chen et al. 2019; Dou et al. 2011). Indeed, the V_{micro} in pristine *TEOS_70* is considerably smaller in comparison with other silicas (Table 2). For *TEOS/β-CD_70*, *TEOS/CPTES(5:1)_70*, and *TEOS/CPTES/β-CD(5:1)_70* silicas benzene adsorption could be affected by the pore configuration as well as surface chemistry. Interestingly, that *TEOS/β-CD_70* silica demonstrated higher benzene adsorption capacity than modified *TEOS/CPTES(5:1)_70* and *TEOS/CPTES/β-CD(5: 1)_70* ones at relative pressure increasing. Perhaps, bulk functional groups on the surface of modified silicas hinder the diffusion of benzene molecules and the pore filling (Ncube et al. 2017; Taba 2010). However, enlarged benzene adsorption was observed on *TEOS/CPTES/β-CD(5:1)_70* silica in comparison with *TEOS/CPTES(5: 1)_70* under higher relative vapor pressures. Taking into account their similar textural properties, one of the plausible explanations for this effect is the existence of cyclic oligosaccharide moieties as specific adsorption centers on the surface of *TEOS/CPTES/β-CD(5:1)_70* material. In general, adsorption of benzene on synthesized sol–gel silicas reached 2–3 mmol/g (130–285 mg/g), and this value is close to benzene adsorption on other microporous silica composites at 25 °C (Adebayo et al. 2020; Chen et al. 2019; Dou et al. 2011; Pendleton 2000). Furthermore, the amount of adsorbed aromatic compound is higher than obtained for molecular sieve silica and zeolite, amino-modified KIT-6 mesoporous silicas, and natural silicate clay minerals (El-Safty 2003; Lu et al. 2020; Ncube et al. 2017). Although synthesized silicas exhibit lower adsorption capacities than for carbon materials (Fu et al. 2011), their use as sorbents permits to resolve activated carbon's frequently encountered problems, such as pore clogging, hygroscopicity, non-selectivity, high costs for regeneration and relatively poor mechanical strength.

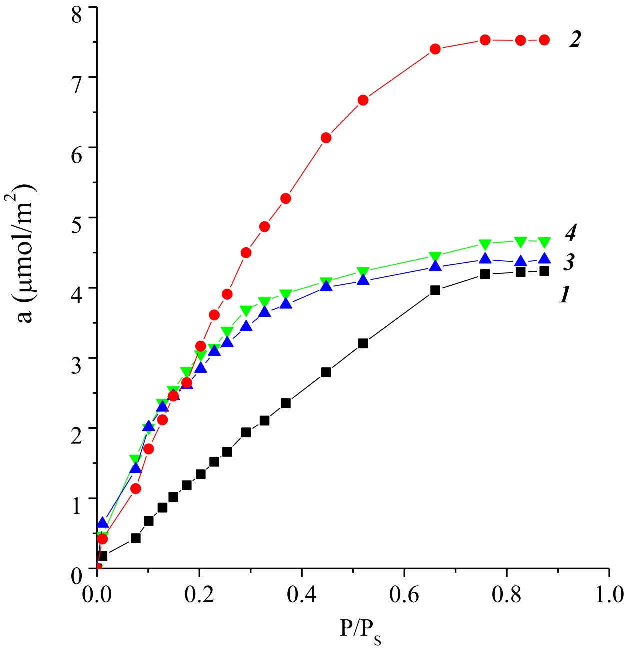

Fig. 10 Gas-phase adsorption isotherms of benzene on *TEOS_70* (curve *1*), *TEOS/β-CD_70* (curve *2*), *TEOS/CPTES(5: 1)_70* (curve *3*), and *TEOS/CPTES/β-CD(5: 1)_70* (curve *4*) silicas

Liquid-phase aromatics extraction by synthesized sol–gel silicas differs from gas-phase adsorption behavior. Sorption experiments were carried out to study the effect of chloropropyl and cyclodextrin groups' attendance in silica matrix on phenol uptakes from aqueous solutions. To estimate equilibrium sorption time required for the uptake of phenol from aqueous solutions by investigated silica materials, time-dependent sorption studies were performed, whereas theirs sorption ability was characterized in terms of sorption isotherms (Fig. 9).

The uptake of phenol was rapid and equilibrium was reached after 1 h for *TEOS_70*, *TEOS/β-CD_70*, and *TEOS/CPTES(5:1)_70* silicas or above 2 h for *TEOS/CPTES/β-CD(5:1)_70* sample (Fig. 11a). It is known that unmodified silicas do not have good sorption affinity to phenol in aqueous medium (El-Safty 2003). There are two different types of adsorption sites on the surface of pristine silica: polar silanol groups with high energy of adsorption and less polar siloxane groups with low adsorption energy. As can be seen from isotherm curves (Fig. 11b), the uptake of phenol from aqueous solutions on *TEOS_70* silica is close to its sorption behavior on *TEOS/β-CD_70* material unlike high adsorption of aromatics from gas phase on the last one. It seems that the presence of specific adsorption sites on the surface of silica but not its pore structure determines sorption performance of material in water liquid medium. To improve sorption properties toward phenol, silica surface is often modified with hydrophobic functional groups (Fu et al. 2011; Kim et al. 2014; Qin et al. 2013). Compared with *TEOS_70* and *TEOS/β-CD_70* silicas, *TEOS/CPTES(5:1)_70* and *TEOS/CPTES/β-CD(5:1)_70* materials with covalently attached 3-chloropropyl and cyclic oligosaccharide groups have high sorption capacity toward phenol. Equilibrium sorption experiments showed clearly that TEOS/CPTES solids, synthesized by sol-gel hydrolysis and condensation, present stronger affinity to aromatics. Interestingly, β-CD-containing silica demonstrates higher phenol sorption behavior in water at equilibrium concentration nearby 10 mmol/L than silica with only surface 3-chloropropyl groups. The difference in sorption capacities of these silicas corresponds to the amount of attached β-cyclodextrin moieties according to the results of chemical analysis (0.012 μmol/m^2). This can be directly ascribed to the formation of inclusion complexes with phenol inside an accessible cavity of β-CD, immobilized on the surface of silicas. Various sorbents were used to treat phenol-containing aqueous solutions, such as polymers, modified bentonites, apatite, hematite, carbon nanotubes, low-cost natural adsorbents, and activated carbons, as the most widely utilized materials (Busca et al. 2008). In comparison with these materials, synthesized sol–gel silicas do not show outstanding sorption performance toward phenol (1–3 mg/g). Nevertheless, they were obtained via a simple sol–gel technique in one-pot synthesis. Synthesized CD-containing silicas are hydrolytically stable materials with high surface area and specific adsorption sites on them. The proposed approach may be considered for industrial preparation of sorbents for separation and removal of aromatic compounds from aqueous media.

Conclusions

The present study demonstrates a simple time-saving method of porous organosilicas (with chloropropyl and/or β-cyclodextrin groups) obtaining via sol–gel synthesis realized in mild condition without using toxic solvents and costly templates. The effect of various synthesis conditions, including relative reagent concentration, temperature, and the hydrothermal treatment on the structure and composition of silicas was investigated. All materials were characterized in details by a number of physico-chemical methods. Increasing amount of functional precursor as well as adding of oligosaccharide in sol–gel reaction mixture decelerated gelation rate drastically, which influenced on the porous structure of synthesized silicas. Rising temperatures of sol–gel reaction accelerated the gelling and successful attaching of 3-chloropropyl and β-cyclodextrin moieties on the surface of silicas. At the same time, hydrothermal treatment application did not lead to more effective modification of silica surface, but its prolongation affected in irreversible

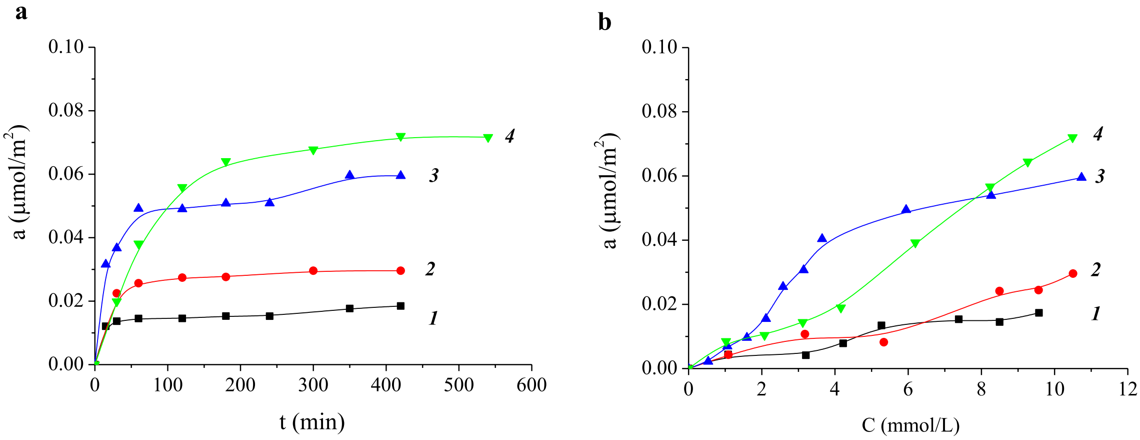

Fig. 11 Kinetic graphs (**a**) and isotherms (**b**) of phenol sorption on *TEOS_70* (curve *1*), *TEOS/β-CD_70* (curve *2*), *TEOS/CPTES(5: 1)_70* (curve *3*), and *TEOS/CPTES/β-CD(5: 1)_70* (curve *4*) silicas

changes in chemical structure of materials. Hydrolytically unstable Si–O–C linkages are formed because of hydrolysis and polycondensation of tetraethyl orthosilicate and β-cyclodextrin, whereas stronger C–O–C linkages are formed as a result of 3-chloropropyl)triethoxysilane adding. Hybrid silica obtained via acidic hydrolysis of the blend of two silanes with molar ratio 5:1 and β-cyclodextrin adding at temperature 70 °C demonstrates developed porosity and content of surface oligosaccharide groups equal to 4.83 μmol/g. Silica obtained at optimal synthesis conditions with high surface area and tailored pore structure shows good removal efficiency toward aromatic compounds even at moderate quantities of attached organic moieties. The results of sorption study indicate that gas-phase adsorption's behavior undergoes by silica pore structure as well as surface chemistry, whereas the presence of specific adsorption sites on the surface of silica determines sorption performance of material in water liquid medium. An important influence of cyclic oligosaccharide additive on the structure and further sorption processes occurring on the surface of synthesized sol–gel silicas was demonstrated.

Acknowledgements The data of this study corresponded in part at the International conference "Nanomaterials: Applications and Properties" (NAP-2013). The full research was presented at the International conference "Nanotechnology and Nanomaterials (NANO-2021)" and submitted as the research article to a special issue.

Funding We received no funding for this study.

Compliance with ethical standards

Conflict of interest We have no competing interests.

References

Adam F, Osman H, Hello KM (2009) The immobilization of 3-(chloropropyl) triethoxysilane onto silica by a simple one-pot synthesis. J Colloid Interface Sci 331(1):143–147

Adebayo BO, Lawson S, Rownaghi AA, Rezaei F (2020) Analysis of equilibrium and dynamic adsorption of benzene vapor over unimodal and bimodal silica-based mixed-metal oxides. Chem Eng J 396:125273

Al-Oweini R, El-Rassy H (2010) Surface characterization by nitrogen adsorption of silica aerogels synthesized from various $Si(OR)_4$ and $R''Si(OR')_4$ precursors. Appl Surf Sci 257(1):276–281

Attol DH, Mihsen HH (2020) Synthesis of silica-salen derivative from rice husk ash and its use for extraction of divalent metal ions Co (II), Ni (II) and Cu (II). Indonesian J Chem 20(1):16–28

Bagherzadeh M, Zare M, Salemnoush T, Ozkar S, Akbayrak S (2014) Immobilization of dioxomolybdenum (VI) complex bearing salicylidene 2-picoloyl hydrazone on chloropropyl functionalized SBA-15: A highly active, selective and reusable catalyst in olefin epoxidation. Appl Catal A Gen 475:55–62

Barrett EP, Joyner LG, Halenda PP (1951) The determination of pore volume and area distributions in porous substances. I. Computations from nitrogen isotherms. J Am Chem Soc 73(1):373–380

Bellamy LJ (1975) The infra-red spectra of complex molecules. Wiley, New York

Busca G, Berardinelli S, Resini C, Arrighi L (2008) Technologies for the removal of phenol from fluid streams: a short review of recent developments. J Hazard Mater 160(2–3):265–288

Chen Q, Zhu R, Deng L et al (2019) One-pot synthesis of novel hierarchically porous and hydrophobic Si/SiOx composite from natural palygorskite for benzene adsorption. Chem Eng J 378:122131

Daoud WA, Xin JH, Tao X (2006) Synthesis and characterization of hydrophobic silica nanocomposites. Appl Surf Sci 252(15):5368–5371

Darmawan A, Rasyid SA, Astuti Y (2021) Modification of the glass surface with hydrophobic silica thin layers using tetraethylorthosilicate (TEOS) and trimethylchlorosilane (TMCS) precursors. Surf Int Anal 53(3):305–313

De Conto JF, Oliveira MR, Oliveira MM, Brandão TG, Campos KV, Santana CC, Egues SM (2018) One-pot synthesis and modification of silica nanoparticles with 3-chloropropyl-trimethoxysilane assisted by microwave irradiation. Chem Eng Commun 205(4):533–537

Dou B, Li J, Wang Y, Wang H, Ma C, Hao Z (2011) Adsorption and desorption performance of benzene over hierarchically structured carbon–silica aerogel composites. J Hazard Mater 196:194–200

Edeler D, Draca D, Petkovic V, Natalio F, Maksimovic-Ivanic D, Mijatovic S, Kaluđerović GN (2019) Impact of the mesoporous silica SBA-15 functionalization on the mode of action of $Ph_3Sn(CH_2)_6OH$. Mater Sci Eng C 100:315–322

El-Nahhal IM, El-Ashgar NM (2007) A review on polysiloxane-immobilized ligand systems: synthesis, characterization and applications. J Organomet Chem 692(14):2861–2886

El-Safty SA (2003) Sorption and diffusion of phenols onto well-defined ordered nanoporous monolithic silicas. J Colloid Interface Sci 260(1):184–194

Fagerlund G (1973) Determination of specific surface by the BET method. Mater Constr 6(3):239–245

Fu J, He Q, Wang R, Liu B, Hu B (2011) Comparative study of phenol compounds adsorption on mesoporous sieves with different degrees of modification. Colloids Surf A Physicochem Eng Asp 375(1–3):136–140

Ghahremani M, Davarpanah J, Rezaee P, Davoodi G (2020) Synthesis of phthalazine compounds using heterogeneous base catalyst based on silica nanoparticles obtained from rice husk. Res Chem Intermed 46(5):2683–2704

Ghorbani S, Parnian R, Soleimani E (2021) Pd nanoparticles supported on pyrazolone-functionalized hollow mesoporous silica as an excellent heterogeneous nanocatalyst for the selective oxidation of benzyl alcohol. J Organomet Chem 952:122025

Guo QX, Luo SH, Liu YC (1998) Substituent effects on the driving force for inclusion complexation of α-and β-cyclodextrin with monosubstituted benzene derivatives. J Incl Phenom Mol Recognit Chem 30(2):173–182

Ha TJ, Choi SG, Jung SB, Yu BG, Park H-H (2008) The improvement of mechanical and dielectric properties of ordered mesoporous silica film using TEOS-MTES mixed silica precursor. Ceram Int 34(4):947–951

Hello KM, Fahad NG (2019) In-situ nitrous acid generation over silica imidazole catalyst for dyes production. Bull Chem React Eng Catal 14(2):247–259

Hello KM, Ibrahim AA, Shneine JK, Appaturi JN (2018) Simple method for functionalization of silica with alkyl silane and organic ligands. S Afr J Chem Eng 25:159–168

Hoffmann F, Cornelius M, Morell J, Froba M (2006) Silica-based mesoporous organic-inorganic hybrid materials. Angew Chem Int Ed 45(20):3216–3251

Jal PK, Patel S, Mishra BK (2004) Chemical modification of silica surface by immobilization of functional groups for extractive concentration of metal ions. Talanta 62(5):1005–1028

Jiang C, Liu W, Yang M, He S, Xie Y, Wang Z (2018) Synthesis of superhydrophobic fluoro-containing silica sol coatings for cotton textile by one-step sol–gel process. J Sol-Gel Sci Technol 87(2):455–463

Jiang X, Tang X, Tang L, Zhang B, Mao H (2019) Synthesis and formation mechanism of amorphous silica particles via sol–gel process with tetraethylorthosilicate. Ceram Int 45(6):7673–7680

Kfoury M, Landy D, Fourmentin S (2018) Characterization of cyclodextrin/volatile inclusion complexes: a review. Molecules 23(5):1204

Kim SW, Bae SJ, Hyeon T, Kim BM (2001) Chiral proline-derivative anchored on mesoporous silicas and their application to the asymmetric diethylzinc addition to benzaldehyde. Microporous Mesoporous Mater 44:523–529

Kim YH, Lee B, Choo KH, Choi SJ (2014) Adsorption characteristics of phenolic and amino organic compounds on nano-structured silicas functionalized with phenyl groups. Microporous Mesoporous Mater 185:121–129

Landy D, Fourmentin S, Salome M, Surpateanu G (2000) Analytical improvement in measuring formation constants of inclusion complexes between β-cyclodextrin and phenolic compounds. J Incl Phenom Macrocycl Chem 38(1):187–198

Lanitou O, Dimotikali D, Yannakopoulou E, Papadopoulos K (2007) Studies on the catalytic activity of novel hybridized chiral organo-inorganic catalysts for epoxidation and alkylation reactions. Chem Eng J 134(1–3):72–77

Leboda R, Mendyk E (1991) Hydrothermal modification of porous structure of silica adsorbents. Mater Chem Phys 27(2):189–212

Lu Y, Li Y, Liu D, Ning Y, Yang S, Yang Z (2020) Adsorption of benzene vapor on natural silicate clay minerals under different moisture contents and binary mineral mixtures. Colloids Surf A Physicochem Eng Asp 585:124072

Lubda D, Cabrera K, Nakanishi K, Lindner W (2003) Monolithic silica columns with chemically bonded β-cyclodextrin as a stationary phase for enantiomer separations of chiral pharmaceuticals. Anal Bioanal Chem 377(5):892–901

Mah SK, Chung IJ (1995) Effects of dimethyldiethoxysilane addition on tetraethylorthosilicate sol-gel process. J Non Cryst Solids 183(3):252–259

McBain JW, Bakr AM (1926) A new sorption balance1. J Am Chem Soc 48(3):690–695

Ncube T, Kumar Reddy KS, Al Shoaibi A, Srinivasakannan C (2017) Benzene, toluene, m-xylene adsorption on silica-based adsorbents. Energy Fuels 31(2):1882–1888

On DT, Desplantier-Giscard D, Danumah C, Kaliaguine S (2001) Perspectives in catalytic applications of mesostructured materials. Appl Catal A Gen 222:299–357

Pendleton P (2000) Temperature influence of benzene adsorption by a microporous silica. J Colloid Interface Sci 227(1):227–236

Perez-Quintanilla D, Del Hierro I, Fajardo M, Sierra I (2006) 2-Mercaptothiazoline modified mesoporous silica for mercury removal from aqueous media. J Hazard Mater 134(1–3):245–256

Ponchel A, Abramson S, Quartararo J, Bormann D, Barbaux Y, Monflier E (2004) Cyclodextrin silica-based materials: advanced characterizations and study of their complexing behavior by diffuse reflectance UV–Vis spectroscopy. Microporous Mesoporous Mater 75(3):261–272

Qin G, Yao Y, Wei W, Zhang T (2013) Preparation of hydrophobic granular silica aerogels and adsorption of phenol from water. Appl Surf Sci 280:806–811

Rajbanshi B, Saha S, Das K, Barman BK, Sengupta S, Bhattacharjee A, Roy MN (2018) Study to probe subsistence of host-guest inclusion complexes of α and β-cyclodextrins with biologically potent drugs for safety regulatory dischargement. Sci Rep 8(1):1–20

Richer R, Mercier L (2001) Direct synthesis of functional mesoporous silica by neutral pH nonionic surfactant assembly: factors affecting framework structure and composition. Chem Mater 13(9):2999–3008

Roik NV, Belyakova LA (2011) Interaction of supramolecular centers of silica surface with aromatic amino acids. J Colloid Interface Sci 362(1):172–179

Roik NV, Belyakova LA, Trofymchuk IM, Dziazko MO, Oranska OI (2017) Mesoporous silicas with covalently immobilized β-cyclodextrin moieties: synthesis, structure, and sorption properties. J Nanopart Res 19(9):1–16

Sahoo S, Kumar P, Lefebvre F, Halligudi SB (2007) Immobilized chiral diamino Ru complex as catalyst for chemo-and enantioselective hydrogenation. J Mol Catal A Chem 273(1–2):102–108

Sing KS (1989) The use of gas adsorption for the characterization of porous solids. Colloids Surf 38(1):113–124

Sobh HS, Mihsen HH (2019) Synthesis of functionalized silica from rice husks containing CI end group. Baghdad Sci J 16(4):886–891

Szaniszlo N, Fenyvesi E, Balla J (2005) Structure-stability study of cyclodextrin complexes with selected volatile hydrocarbon contaminants of soils. J Incl Phenom Macrocycl Chem 53(3–4):241–248

Szejtli J (1998) Introduction and general overview of cyclodextrin chemistry. Chem Rev 98(5):1743–1754

Taba P (2010) Adsorption of water and benzene vapour in mesoporous materials. Makara J Sci

Thommes M (2010) Physical adsorption characterization of nanoporous materials. Chem Ing Tech 82(7):1059–1073

Thommes M, Kaneko K, Neimark AV, Olivier JP, Rodriguez-Reinoso F, Rouquerol J, Sing KS (2015) Physisorption of gases, with special reference to the evaluation of surface area and pore size distribution (IUPAC Technical Report). Pure Appl Chem 87(9–10):1051–1069

Toufaily J, Koubaissy B, Kafrouny L, Hamad H, Magnoux P, Ghannam L, Karout A, Hazimeh H, Nemra G, Hamieh M, Ajouz N, Hamieh T (2013) Functionalization of SBA-15 materials for the adsorption of phenols from aqueous solution. Centr Eur J Eng 3(1):126–134

Trofymchuk IM, Belyakova LA, Grebenyuk AG (2011) Study of complex formation between β-cyclodextrin and benzene. J Incl Phenom Macrocycl Chem 69(3–4):371–375

Trofymchuk I, Roik N, Belyakova L (2017) Structural variety and adsorptive properties of mesoporous silicas with immobilized oligosaccharide groups. Nanoscale Res Lett 12(1):1–14

Udayakumar S, Son YS, Lee MK, Park SW, Park DW (2008) The synthesis of chloropropylated MCM-41 through co-condensation technique: the path finding process. Appl Catal A Gen 347(2):192–199

Vansant EF, Van Der Voort P, Vrancken KC (1995) Characterization and chemical modification of the silica surface. Elsevier

Voorhees PW (1985) The theory of Ostwald ripening. J Stat Phys 38(1):231–252

Wagh PB, Ingale SV (2002) Comparison of some physico-chemical properties of hydrophilic and hydrophobic silica aerogels. Ceram Int 28(1):43–50

Wang F, Liu J, Luo Z, Zhang Q, Wang P, Liang X, Li C, Chen J (2007) Effects of dimethyldiethoxysilane addition on the sol–gel process of tetraethylorthosilicate. J Non Cryst Solids 353(3):321–326

Wang F, Liu J, Yang H, Luo Z, Lv W, Li C, Qing S (2008a) Spherical particles from tetraorthosilicate (TEOS) sol-gel process with dimethyldiethoxysilane (DDS) and diphenyldiethoxysilane (DPDS) addition. J Non-Cryst Solids 354(45–46):5047–5052

Wang J, Huang L, Xue M, Liu L, Wang Y, Gao L, Zhu J, Zou Z (2008b) Developing a novel fluorescence chemosensor by self-assembly of Bis-Schiff base within the channel of mesoporous

SBA-15 for sensitive detecting of Hg2+ ions. Appl Surf Sci 254(17):5329–5335

Wei F, Yang JY, Gao L, Gu FN, Zhu JH (2009) Capturing nitrosamines in tobacco-extract solution by hydrophobic mesoporous silica. J Hazard Mater 172(2–3):1482–1490

Weitkamp J, Hunger M, Rymsa U (2001) Base catalysis on microporous and mesoporous materials: recent progress and perspectives. Microporous Mesoporous Mater 48(1–3):255–270

Wen J, Wilkes GL (1996) Organic/inorganic hybrid network materials by the sol−gel approach. Chem Mater 8(8):1667–1681

Wieszczycka K, Staszak K, Wozniak-Budych MJ, Litowczenko J, Maciejewska BM, Jurga S (2021) Surface functionalization–The way for advanced applications of smart materials. Coord Chem Rev 436:213846

Xia T, Yang H, Li J, Sun C, Lei C, Hu Z, Zhang Y (2019) Synthesis and physicochemical characterization of silica aerogels by rapid seed growth method. Ceram Int 45(6):7071–7076

Xu YQ, Cao Y, Xia ZN (2012) Microwave radiation one-pot synthesis of chloropropyl-functionalized mesoporous MCM-41. J Cent South Univ 19(8):2130–2135

Yang HS, Choi SY, Hyun SH, Park HH, Hong JK (1997) Ambient-dried low dielectric SiO2 aerogel thin film. J Non Cryst Solids 221(2–3):151–156

Zhang X, Wu Y, He S, Yang D (2007) Structural characterization of sol-gel composites using TEOS/MEMO as precursors. Surf Coat Technol 201(12):6051–6058